
Knowledge-enhanced Relation Graph and Task Sampling for Few-shot Molecular Property Prediction

Zeyu Wang¹ Tianyi Jiang¹ Yao Lu¹ Xiaoze Bao² Shanqing Yu¹
Bin Wei² Qi Xuan^{1*}

¹Institute of Cyberspace Security, Zhejiang University of Technology

²the College of Pharmaceutical Science & Collaborative Innovation Center of Yangtze River
Delta Region Green Pharmaceuticals, Zhejiang University of Technology
vencent_wang@outlook.com, xuanqi@zjut.edu.cn

Abstract

Recently, few-shot molecular property prediction (FSMPP) has garnered increasing attention. Despite impressive breakthroughs achieved by existing methods, they often overlook the inherent many-to-many relationships between molecules and properties, which limits their performance. For instance, similar substructures of molecules can inspire the exploration of new compounds. Additionally, the relationships between properties can be quantified, with high-related properties providing more information in exploring the target property than those low-related. To this end, this paper proposes a novel meta-learning FSMPP framework (KRGTS), which comprises the **K**nowledge-enhanced **R**elation **G**raph module and the **T**ask **S**ampling module. The knowledge-enhanced relation graph constructs the molecule-property multi-relation graph (MPMRG) to capture the many-to-many relationships between molecules and properties. The task sampling module includes a meta-training task sampler and an auxiliary task sampler, responsible for scheduling the meta-training process and sampling high-related auxiliary tasks, respectively, thereby achieving efficient meta-knowledge learning and reducing noise introduction. Empirically, extensive experiments on five datasets demonstrate the superiority of KRGTS over a variety of state-of-the-art methods. The code is available in <https://github.com/Vencent-Won/KRGTS-public>.

1 Introduction

Molecular property prediction (MPP), aiming to predict the physicochemical properties and biological activity of molecules, is a crucial task in drug discovery. In the past, MPP is expensive, time-consuming, and risky by wet lab experiments. With the advancement of machine learning, lots of MPP models have been developed to ameliorate this situation. For example, deep learning methods showed great potential, such as [1, 2, 3] model molecules as text or graph data to explore properties with language models or graph neural networks. However, as the data dependency, limited annotated data hinders MPP models in practical applications. It is essentially a few-shot learning problem.

Few-shot learning refers to learning from limited samples with supervised information [4, 5]. Although the few-shot learning methods are widely studied in computer vision and natural language processing [6, 7], it is still under-explored in MPP. In recent years, several few-shot learning methods, as are listed in Table 1, have been introduced to MPP. Specifically, IterRefLSTM [8] is a few-shot learning framework that combines the iterative refinement long short-term memory and graph convolution network. Meta-MGNN [9] utilizes the self-supervised atom-bond prediction tasks and self-attentive property weight learning module with episodic training diagram in meta-learning. However, these methods overlook the correlation between molecules, meaning that labeled molecules

Table 1: The comparison of few-shot molecular property prediction methods.

Methods	meta-learning	molecule-property relation	molecule-molecule relation	meta-training task sampler	auxiliary task sampler
IterRefLSTM [8]	-	-	-	-	-
Meta-MGNN [9]	✓	-	-	random sampling	-
PAR [10]	✓	-	property aware relation	random sampling	-
HSL-RG [11]	✓	-	molecular embedding similarity	random sampling	-
PG-DERN [12]	✓	-	molecular embedding similarity	random sampling	-
GS-Meta [13]	✓	✓	molecular embedding similarity	optimized sampler	random sampling
KRGTS	✓	✓	molecular substructure similarity	optimized sampler with task relationships	optimized sampler

can offer valuable information for unlabeled ones. PAR [10] emphasized the importance of relationships between different molecules and proposed the property-aware relation between molecules. HSL-RG [11] and PG-DERN [12] constructed molecular relation graphs with molecular representations to capture information from support molecules. Furthermore, GS-Meta [13] took account of the correlation of properties and developed a contrastive learning meta-training task sampler and the molecule-property relation graph (MPRG) which consists of auxiliary properties, target properties, and molecules. Although these methods noticed the correlation between the molecules, graph embedding-based similarity of molecules may be sensitive to model initialization and may not be as accurate as direct structure comparisons, such as comparing molecular scaffold topology or functional group types. Also, they overlooked the fine-grained molecular relationships and the quantification of the relationships between molecular properties. As is known to all, one of the key factors influencing molecular properties is the molecular substructure, including scaffolds and functional groups [14, 15, 16], which serve as essential indicators in laboratory research. Moreover, as for the correlation between properties, the low-related auxiliary properties generally have fewer contributions to target property prediction than high-related properties, which is also reflected in transfer learning [17]. And, excessive low-related properties will introduce additional computation, information redundancy and make the model smooth, thereby affecting its generalization.

To handle these problems, this paper delves into fine-grained relationships of molecules and the qualification of relationships between properties, proposing a novel FSMPP framework that comprises the **Knowledge-enhanced Relation Graph** module and the **Task Sampling** module (KRGTS). Specifically, the knowledge-enhanced relation graph module constructs the molecule-property multi-relation graph (MPMRG) incorporating substructure (scaffold and functional group) similarities of molecules and property information, effectively capturing the many-to-many relationships between molecules and properties. Given the scale of MPMRG, KRGTS samples target-centered subgraphs from MPMRG, comprising a target property, molecules, and auxiliary properties, to train the FSMPP model. The task sampling module comprises a meta-training task sampler and an auxiliary task sampler. Among them, the auxiliary task sampler is designed to select high-related auxiliary properties for the target-centered subgraph. Due to the imbalance of data and the connectivity of different subgraphs, it is important to sample suitable meta-training tasks, aiming to effectively accumulate meta-knowledge. The meta-training task sampler utilizes the properties similarity guidance to schedule the training process by sampling subgraphs with different target tasks and is optimized through subgraph-to-subgraph contrastive learning, minimizing the discrepancy between the same target-centered subgraphs while maximizing the discrepancy between different ones. The contributions are summarized as follows:

- This paper utilizes the scaffold similarity and functional group similarity with the property information to construct MPMRG, which could effectively capture the many-to-many correlations between molecules and properties.
- This paper first proposes to sample the high-related properties as the auxiliary properties to explore the target molecular property. Correspondingly, this paper develops the task sampler module consisting of a meta-training task sampler and an auxiliary task sampler.
- Extensive experiments on FSMPP datasets demonstrate the superiority of KRGTS over various state-of-the-art methods. Furthermore, the ROC-AUC of the Tox21 reaches 87.62%.

2 Related Work

2.1 Molecular Property Prediction

Molecular property prediction refers to predicting the physicochemical properties and biological activity of molecules, which plays an important role in virtual screening, drug design, and property

optimization process [18]. The mainstream methods of MPP can be divided as molecular descriptors-based methods, Simplified Molecular Input Line Entry Specification (SMILES) based methods, and graph (2D&3D) based methods [18, 19]. Among them, molecular descriptors-based methods are traditional methods that explore the relationship between properties and the topology or characteristic description such as molecular fingerprint [20, 21]. However, the molecular fingerprint can not capture the multi-scale information and 3D conformation information. With the progression of deep learning, SMILES-based methods and graph-based methods showed tremendous potential. SMILES-based methods generally apply the sequence model to learn the molecular representation [1], which can effectively encode the atoms and bonds. While compared to the molecular graph, the SMILES lacks structure information and can not distinguish the stereoisomers. Molecules and graph data are highly compatible as the atoms and bonds can be converted to the nodes and edges. There are lots of graph-based methods that encode the molecules with graph neural networks such as the 2D graph [22], the 3D graph [23] and multi-view methods [24, 25]. Considering the superiority of graph neural network, KRGTS models molecules as graphs to obtain comprehensive molecular representations.

2.2 Few-shot Molecular Property Prediction

Few-shot learning has achieved excellent success in computer vision and natural language processing but is still in its fancy in the field of MPP. Recent efforts have been made to release this situation. [9] proposed that limited data hinder the deep learning application in MPP and developed Meta-MGNN that consists of molecular self-supervised modules and self-attentive task weights module with meta-learning. Taking the relationships of molecules into account, PAR [10] introduced the property-aware molecular relation and an adaptive relation learning module. HSL-RG [11] utilized the graph kernel to construct relation graphs, enabling the global communication of molecular structural knowledge across neighboring molecules. GS-Meta [13] proposed the gap in the consideration of properties relationships and introduced the meta-training task sampler to achieve the effective learning of meta-knowledge. Although these methods have noticed the importance of the relationships between molecules and properties, they overlook the fine-grain relationships such as the substructures (functional groups and scaffolds) relation of different molecules. The graph neural network and graph kernel methods generally pay attention to the global feature and similarity, which can not effectively capture the local feature. Furthermore, they neglect the impact of the relationships of auxiliary properties and different target properties. Additionally, MTA [26] proposed a task augmentation strategy that constructs new samples with highly relevant motifs. However, different from other data (such as images), the properties of virtual molecules are uncertainty factors. To this end, this paper constructs the MPMRG with the substructure similarity of molecules with the property information to capture the auxiliary information provided by annotated molecules. Moreover, to reasonably utilize the information on auxiliary properties that have different relationships with target properties, this paper introduced the auxiliary task sampler to sample the high-related auxiliary properties.

3 Preliminaries

Molecule-Property Relation Graph (MPRG). A molecule-property relation graph is defined as a graph $G = (V, T, E, B)$, where V is the molecule set, T is the property set, $E = \{(i, \tau) | i \in V, \tau \in T\}$ denotes the molecular property information, and B is the edge weight set. Also, the edge weight set $B = \{b_{i,\tau} | (i, \tau) \in E\}$ indicates the label of the molecule i for property τ , where $b \in \{0, 1, 2\}$ (0 is inactive, 1 is active, 2 is unknown). Moreover, there is no relation between molecules.

Molecule-Property Multi-Relation Graph (MPMRG). Compared to the molecule-property graph, the molecule-property multi-relation graph not only encompasses molecular properties information but also incorporates relationships among different molecules. Consequently, the molecule-property multi-relation graph can be regarded as a multiplex graph which is a multi-layer view of a graph $M = (V, T, R, \mathbb{M})$. Here, V and T signify the molecules and properties within the molecule-property relation graph, constituting sets of supra-nodes instantiated separately in each layer of the multiplex network. R represents the set of relations, encompassing connections between diverse molecules and from molecules to properties. These relations in the molecule-property relation graph are the foundation for each layer graph within the multiplex network. $\mathbb{M} = \{G^r\}_{r \in R}$ is the set of layer graphs that include several relation graphs.

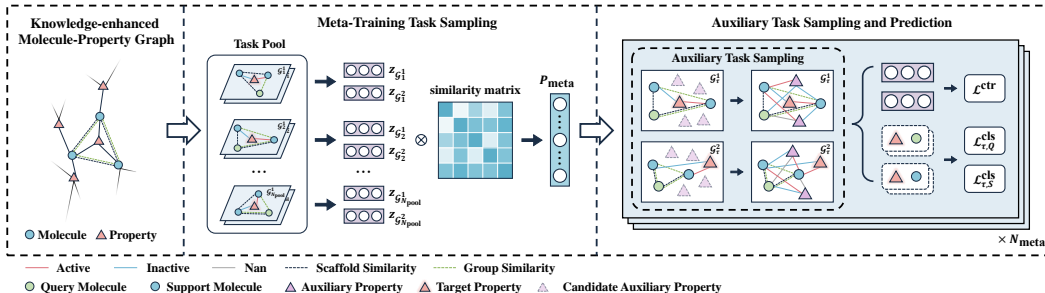


Figure 1: The pipeline of KRGTS in 2-way 1-shot setting.

Problem Definition. The FSMPP aims to develop a model with the generalization ability to new tasks through training with only a few annotated data. In line with [9], the FSMPP is conducted on a set of tasks T which corresponds to the N_t molecular properties. Then, the task set can be divided into T_{train} and T_{test} , corresponding to the training tasks and testing tasks. Generally, the MPP involves qualitative analysis tasks with two classes. Accordingly, the FSMPP task τ can be formulated as a 2-way K -shot classification task $\{S_\tau, Q_\tau\}$, where $S_\tau = \{(v_i, y_{i,\tau})\}_{i=1}^{2K}$ is a set of labeled support molecules, $Q_\tau = \{(v_i, y_{i,\tau})\}_{i=1}^{N_Q}$ is a set of query molecules.

4 Methodology

4.1 Overview

Figure 1 describes the pipeline of KRGTS in 2-way 1-shot setting. Given a FSMPP dataset, one can mainly utilize the substructure similarity of molecules and properties information to construct the knowledge-enhanced molecule-property relation graph, which can be regarded as a MPMRG. Considering the scale of the MPMRG, KRGTS adopts the episodic training paradigm as Meta-MGNN [9]. Based on the contrastive learning mechanism, one can randomly sample a task pool $\{(\mathcal{G}_\tau^1, \mathcal{G}_\tau^2)\}_{\tau=1}^{N_{pool}}$, consisting of pairwise subgraphs of target tasks, where target-centered subgraph \mathcal{G}_τ consists of support set S_τ and query set Q_τ . To effectively accumulate meta-knowledge across different meta-training tasks, the meta-training task sampler schedules the training process by sampling a batch of meta-training tasks $\{(\mathcal{G}_\tau^1, \mathcal{G}_\tau^2)\}_{\tau=1}^{N_{meta}}$. Moreover, to capture auxiliary task information and reduce information redundancy, the auxiliary task sampler samples high-related auxiliary tasks (known properties) for target tasks (target properties). Then, one can utilize complete subgraphs to learn comprehensive representations of molecules and properties and apply them to predict the target property. And the algorithm and implementation are listed in Appendix B.

4.2 Knowledge-enhanced Molecule-Property Relation Graph

Relation Graph Construction. According to the definition in Section 3, the MPRG can be constructed using molecules and property information. As shown in Figure 2 (A), nodes represent molecules and properties, and edges represent molecular properties. Although this network intuitively includes property information, it ignores the many-to-many relationships between molecules and properties. HSL_RG [11] and GS-Meta [13] propose to utilize molecular representation similarity as molecular similarities to enrich information, these methods not only ignore important fine-grained similarities but also are heavily influenced by model initialization, which can lead to overfitting. Therefore, this paper proposes to augment the molecular property relation network using the similarity of important substructures (scaffolds and functional groups). As illustrated in Figure 2 (B), KRGTS

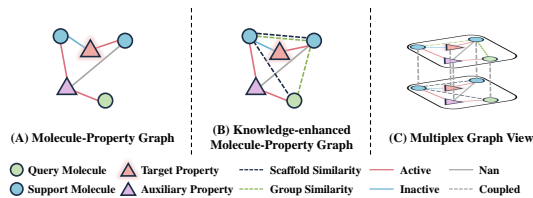


Figure 2: The comparison of molecular-property relation graph and knowledge-enhanced molecule-property graph.

constructs the knowledge-enhanced molecule-property relation graph, which can be regarded as a MPMRG $M = (V, T, R, \mathbb{M})$, where R contains property information and two types of sub-structure similarity between molecules, and $\mathbb{M} = \{G^{\text{Sca}}, G^{\text{Gro}}, G^{\text{Pro}}\}$. $G^{\text{Sca}} = (V, T, E^{\text{Sca}}, B^{\text{Sca}})$, $G^{\text{Gro}} = (V, T, E^{\text{Gro}}, B^{\text{Gro}})$, and $G^{\text{Pro}} = (V, T, E^{\text{Pro}}, B^{\text{Pro}})$ represent the scaffold similarity layer, the functional group similarity layer, and the property layer, where $B^{\text{Sca}} = \{b_{i,j} | (i, j) \in E^{\text{Sca}}\}$ and $B^{\text{Gro}} = \{b_{i,j} | (i, j) \in E^{\text{Gro}}\}$ represent the similarity between molecules, and $b \in [0, 1]$. Moreover, KRGS calculates the scaffold similarity and functional group similarity by molecular fingerprints. RDKit¹ is employed to extract the molecular scaffold and functional groups. The scaffold similarity of molecules i and j can be denoted as:

$$\mathcal{S}_{\text{Sca}}(i, j) = \frac{SF_i \cdot SF_j^T}{2214 - (\neg SF_i) \cdot (\neg SF_j)^T}, \quad (1)$$

where \neg is the negation operator, $SF_i \in \{0, 1\}^{2214}$ is the scaffold fingerprint concatenated by the Morgan fingerprint [27] with the dimension of 2048 and MACCS keys [28] with the dimension of 166. Each bit of the SF_i indicates whether a structure exists, so that, can capture important structural features such as the ring in scaffolds. Similarly, KRGS calculates the functional group similarity:

$$\mathcal{S}_{\text{Gro}}(i, j) = \frac{GF_i \cdot GF_j^T}{49 - (\neg GF_i) \cdot (\neg GF_j)^T}, \quad (2)$$

where $GF_i \in \{0, 1\}^{49}$ corresponds to the set of 49 functional groups defined in RDKit. Each bit of the GF_i indicates whether a functional group exists.

Relation Subgraph Learning. Taking the scale of MPMRG into account, KRGS utilizes the subgraph sampling mechanism with the episodic meta-learning diagram [29]. As shown in Figure 1, each task τ can be formulated as a target-centered subgraph \mathcal{G}_τ with a target property, a query molecule sampled from the query set Q_τ , and $2K$ support molecules in the support set S_τ . To utilize the correlations between known properties and the target property, the auxiliary task sampler is devised to sample N_{auxi} high-related available properties, which are connected to molecules in the subgraph, to assist in predicting the target properties. Then, the subgraph can be denoted as $\mathcal{G}_\tau = (\mathcal{V}, \{\tau \cup T_{\text{auxi}}\}, R, \{G_\tau^{\text{Sca}}, G_\tau^{\text{Gro}}, G_\tau^{\text{Pro}}\})$, where G_τ^{Sca} and G_τ^{Gro} only preserve the top- k similarity relations for each molecule to reduce noise. Moreover, due to the diversity of relation types and the heterogeneity in the subgraph, traditional relation neural networks [30] cannot be directly applied. To address this challenge, KRGS treats the \mathcal{G}_τ as a multiplex graph, composed of relation-specific layer graphs with super nodes linked across relations. As depicted in Figure 2 (C), relation-specific layer graphs correspond to the functional group similarity relation layer with property information $\{G_\tau^{\text{Pro}}, G_\tau^{\text{Gro}}\}$ and the molecular scaffold similarity relation layer with property information $\{G_\tau^{\text{Pro}}, G_\tau^{\text{Sca}}\}$. Subsequently, KRGS independently conducts message-passing on the two layers and concatenates the outputs to obtain the final representation.

Firstly, KRGS utilizes the graph encoder [31], the Embedding layers [32], and radial basis functions [33] to initialize the node (molecules and properties nodes) embedding h_i^0 and edge embedding $h_{i,j}$ (details are in Appendix C). For each relation layer, node embeddings are updated as follows:

$$h_i^l = \text{GNN}(h_i^{l-1}, h_j^{l-1}, h_{i,j} | j \in \mathcal{N}(i)), \quad (3)$$

where h_i^l denotes the embedding of node i after the l -th iteration, $\mathcal{N}(i)$ denotes the neighbor nodes of node i . After L layers aggregation, one can get the node embeddings of two relation layers and concatenate them to get the final node embeddings of \mathcal{G}_τ :

$$z_i = \sigma(\text{MLP}([h_{\text{Sca},i}^L \oplus h_{\text{Gro},i}^L])), \quad (4)$$

where $z_i \in \mathbb{R}^d$ denotes the representation of node i , d is the dimension of subgraph representation, and \oplus is the concatenation operation. Correspondingly, z_τ is the final embedding of the target task τ of \mathcal{G}_τ . To highlight the target task in the subgraph, one can get the subgraph embedding $z_{\mathcal{G}_\tau}$:

$$z_{\mathcal{G}_\tau} = z_\tau + \frac{\sum_{i \in \{\mathcal{V} \cup T_{\text{auxi}}\}} z_i}{|\mathcal{G}_\tau| - 1} \quad (5)$$

¹<https://www.rdkit.org/>

where $|\mathcal{G}_\tau| = |\mathcal{V}| + |\{\tau \cup T_{\text{auxi}}\}|$ denotes the number of nodes in \mathcal{G}_τ . Finally, KRGTS concatenates the embedding of the molecule z_i and the property z_τ to predict target property:

$$\hat{y}_{i,\tau} = f_{\text{clr}}([z_i \oplus z_\tau]), \quad (6)$$

where $\hat{y}_{i,\tau} \in \mathbb{R}^1$ is the prediction, and f_{clr} is a classifier consisting of two layers MLP. Therefore, the loss of support molecules is defined as:

$$\mathcal{L}_{\tau,S}^{\text{cls}} = - \sum_{v_i \in S_\tau} (y_{i,\tau} \log \hat{y}_{i,\tau} + (1 - y_{i,\tau}) \log(1 - \hat{y}_{i,\tau})). \quad (7)$$

Similarly, one can get the loss of query set $\mathcal{L}_{\tau,Q}^{\text{cls}}$.

4.3 Meta-training Task Sampler

As the episodic training diagram showed its success in meta-learning, this training mechanism is gradually adopted for FSMPP. Meta-MGNN [9] and PAR [10] considered meta-training tasks to be equally important and randomly sample meta-training tasks with a fixed probability. On the other hand, GS-Meta designed a meta-training task sampler with reinforcement learning and introduced contrastive learning to augment the task representation learning designs. However, all of them failed to capture the inherent correlation between different tasks. To address these challenges, KRGTS proposes the meta-training task sampler based on two aspects: 1) Each target-centered subgraph with different molecules can be regarded as different views of the target property, so that, should minimize their semantic discrepancy. Correspondingly, the semantics of target-centered subgraphs with different target properties should be enlarged. 2) Capturing the relationships between tasks can guide the sampler to sample meta-training tasks and optimize the meta-knowledge accumulation.

Firstly, according to the setting of contrastive learning, one can randomly sample a task pool $\{(\mathcal{G}_\tau^1, \mathcal{G}_\tau^2)\}_{\tau=1}^{N_{\text{pool}}}$ for sampling, where $\mathcal{G}_\tau^1, \mathcal{G}_\tau^2$ represents the two views of target task τ . Each \mathcal{G}_τ consists of a target task, a query molecule, and $2K$ support molecules, i.e., \mathcal{G}_τ contains $2K+2$ nodes. One can get the subgraph representations $Z_{\text{pool}} \in \mathbb{R}^{2*N_{\text{pool}} \times d}$ with Equation (5) and learn a similarity matrix $A_{\text{pool}} \in \mathbb{R}^{2*N_{\text{pool}} \times 2*N_{\text{pool}}}$ to model the relationships of tasks in the task pool, $A_{\text{pool}}(\tau_1, \tau_2) = \mathcal{S}_{\text{cos}}(z_{\mathcal{G}_{\tau_1}}, z_{\mathcal{G}_{\tau_2}})$, \mathcal{S}_{cos} is the cosine similarity function. Then, one can perform message propagation to enrich the task representations:

$$Z'_{\text{pool}} = \text{ReLU}(A_{\text{pool}} Z_{\text{pool}} W_{\text{pool}}), \quad (8)$$

where $W_{\text{pool}} \in \mathbb{R}^{d \times d}$ is a learnable parameters matrix. Subsequently, one can take the updated representation $z'_{\mathcal{G}_\tau} \in Z'_{\text{pool}}$ as input to get the sampling probability $P_{\text{meta}, \mathcal{G}_\tau}$:

$$P_{\text{meta}, \mathcal{G}_\tau} = f_{\text{meta}}(z'_{\mathcal{G}_\tau}), \quad (9)$$

where f_{meta} consists of L_{meta} layers MLP. The sampling probability of τ is computed as $(P_{\text{meta}, \mathcal{G}_\tau^1} + P_{\text{meta}, \mathcal{G}_\tau^2})/2$. KRGTS selects N_{meta} meta-training tasks with sampling probabilities for each epoch. Moreover, the NT-Xent loss [34] is utilized for subgraph-to-subgraph contrastive learning:

$$\mathcal{L}^{\text{ctr}} = \frac{1}{N_{\text{meta}}} \sum_{\tau=1}^{N_{\text{meta}}} - \log \frac{e^{\mathcal{S}_{\text{cos}}(z_{\mathcal{G}_\tau^1}, z_{\mathcal{G}_\tau^2})/t}}{\sum_{\tau'=1, \tau' \neq \tau}^{N_{\text{meta}}} e^{\mathcal{S}_{\text{cos}}(z_{\mathcal{G}_{\tau'}^1}, z_{\mathcal{G}_{\tau'}^2})/t}}, \quad (10)$$

where t is the temperature parameter. To effectively accumulate meta-knowledge, KRGTS takes the contrastive loss as the reward R_{meta} for optimizing:

$$\phi \leftarrow \phi + lr_{\text{meta}} \nabla_{\phi} P_{\text{meta}}(R_{\text{meta}} - b_{\text{meta}}), \quad (11)$$

where ϕ denotes parameters of the meta-training task sampler module, lr_{meta} is the learning rate of the auxiliary tasks sampler, P_{meta} is the sampling probability of selected meta-training tasks, and b_{meta} is the moving average of reward.

4.4 Auxiliary Task Sampler

Task relevance is not only an important factor in meta-training task scheduling but also plays a pivotal role in relation subgraphs construction. As a crucial source of information within relation subgraphs,

Table 2: ROC-AUC of few-shot molecular property prediction. The best is marked with boldface and the sub-optimal is with underline.

Method	Tox21		SIDER		MUV		ToxCast		PCBA	
	10-shot	1-shot	10-shot	1-shot	10-shot	1-shot	10-shot	1-shot	10-shot	1-shot
Siamese	80.40 _(0.35)	65.00 _(1.58)	71.10 _(4.32)	51.43 _(3.31)	59.96 _(5.13)	50.00 _(0.17)	-	-	-	-
ProtoNet	74.98 _(0.32)	65.58 _(1.72)	64.54 _(0.89)	57.50 _(2.34)	65.88 _(4.11)	58.31 _(3.18)	63.70 _(1.26)	56.36 _(1.54)	64.93 _(1.94)	55.79 _(1.45)
MAML	80.21 _(0.24)	75.74 _(0.48)	70.43 _(0.76)	67.81 _(1.12)	63.90 _(2.28)	60.51 _(3.12)	66.79 _(0.85)	65.97 _(5.04)	66.22 _(1.31)	62.04 _(1.73)
TPN	76.05 _(0.24)	60.16 _(1.18)	67.84 _(0.95)	62.90 _(1.38)	65.22 _(5.82)	50.00 _(0.51)	62.74 _(1.45)	50.01 _(0.05)	-	-
EGNN	81.21 _(0.16)	79.44 _(0.22)	72.87 _(0.73)	70.79 _(0.95)	65.20 _(2.08)	62.18 _(1.76)	63.65 _(1.57)	61.02 _(1.94)	69.92 _(1.85)	62.14 _(1.58)
IterRefLSTM	81.10 _(0.17)	80.97 _(0.10)	69.63 _(0.31)	71.73 _(0.14)	49.56 _(5.12)	48.54 _(3.12)	-	-	-	-
PAR	82.06 _(0.12)	80.46 _(0.13)	74.68 _(0.31)	71.87 _(0.48)	66.48 _(2.12)	64.12 _(1.18)	69.72 _(1.63)	67.28 _(2.90)	70.05 _(0.94)	67.77 _(1.04)
GS-Meta	85.85 _(0.26)	84.32 _(0.89)	83.72 _(0.64)	82.84 _(0.67)	67.11 _(1.95)	64.70 _(2.88)	81.55 _(0.19)	80.03 _(0.26)	72.16 _(0.71)	70.03 _(1.56)
HSL-RG	80.95 _(0.26)	79.65 _(0.22)	74.66 _(0.52)	71.77 _(0.79)	70.38 _(1.35)	67.22 _(1.56)	70.70 _(1.02)	70.06 _(1.05)	-	-
ADKF-IFT	82.42 _(0.60)	77.94 _(0.91)	67.72 _(1.21)	58.69 _(1.44)	98.18 _(3.05)	<u>67.04</u> _(4.86)	72.07 _(0.81)	67.50 _(1.23)	-	-
KRGTS	87.19 _(0.11)	86.49 _(0.18)	84.83 _(0.15)	84.74 _(0.20)	<u>72.63</u> _(1.99)	68.93 _(0.65)	82.61 _(0.52)	81.65 _(0.15)	76.61 _(0.80)	74.15 _(1.10)

Table 3: ROC-AUC obtained with a pre-trained GNN encoder. The best is marked with boldface and the sub-optimal is with underline.

Method	Tox21		SIDER		MUV		ToxCast		PCBA	
	10-shot	1-shot	10-shot	1-shot	10-shot	1-shot	10-shot	1-shot	10-shot	1-shot
Pre-GNN	82.14 _(0.08)	81.68 _(0.09)	73.96 _(0.08)	73.24 _(0.12)	67.14 _(1.58)	64.51 _(1.45)	73.68 _(0.74)	72.90 _(0.84)	-	-
Meta-MGNN	82.94 _(0.10)	82.13 _(0.13)	75.43 _(0.21)	73.36 _(0.32)	68.99 _(1.84)	65.54 _(2.13)	-	-	-	-
Pre-PAR	84.93 _(0.11)	83.01 _(0.09)	78.08 _(0.16)	74.46 _(0.29)	69.96 _(1.37)	66.94 _(1.12)	75.12 _(0.84)	73.63 _(1.00)	73.71 _(0.61)	72.49 _(0.61)
HSL-RG	85.56 _(0.28)	84.09 _(0.20)	78.99 _(0.33)	77.53 _(0.41)	71.26 _(1.08)	68.76 _(1.05)	76.00 _(0.81)	74.40 _(0.82)	-	-
MolFeSCue	85.93 _(0.10)	82.05 _(0.11)	79.08 _(0.14)	73.13 _(0.56)	72.96 _(1.18)	67.32 _(1.08)	76.39 _(1.52)	74.82 _(1.39)	-	-
PG-DERN	85.25 _(0.29)	84.12 _(0.08)	79.62 _(0.32)	77.69 _(0.38)	71.65 _(0.26)	69.66 _(1.02)	75.21 _(0.19)	74.51 _(0.17)	-	-
Pre-GS-Meta	86.91 _(0.41)	86.46 _(0.55)	85.08 _(0.54)	84.45 _(0.26)	70.18 _(1.25)	67.15 _(2.04)	83.81 _(0.16)	81.57 _(0.18)	79.40 _(0.43)	78.16 _(0.47)
Pre-ADKF-IFT	86.06 _(0.35)	80.97 _(0.48)	70.95 _(0.60)	62.16 _(1.03)	95.74 _(0.37)	67.25 _(3.87)	76.22 _(0.13)	71.13 _(1.15)	-	-
Pre-KRGTS	87.62 _(0.29)	87.54 _(0.11)	85.09 _(0.31)	84.61 _(0.16)	<u>74.47</u> _(0.82)	68.69 _(0.60)	84.02 _(0.10)	82.39 _(0.29)	81.59 _(0.30)	81.18 _(0.17)

the information carried by high-related auxiliary tasks is often richer than that from low-related tasks. The low-related auxiliary tasks may introduce extra noise and result in information redundancy. To this end, KRGTS develops a result-oriented auxiliary task sampler with policy gradient [35].

Firstly, for each target property τ , the candidate auxiliary properties set is $T_{\text{can}} = T_{\text{train}} \setminus \tau$. One can get the embedding of the target property subgraph $z_{\mathcal{G}_\tau} \in \mathbb{R}^d$ and the subgraph embeddings of all candidate auxiliary properties $Z_{\text{can}} \in \mathbb{R}^{|T_{\text{can}}| \times d}$. Subsequently, the sampling probability of auxiliary task $\tau_{\text{can}} \in T_{\text{can}}$ is computed as:

$$P_{\text{auxi}, \tau_{\text{can}}} = f_\psi([z_{\mathcal{G}_\tau} \oplus z_{\mathcal{G}_{\tau_{\text{can}}}}]), \quad (12)$$

where f_ψ consists of L_{auxi} layers MLP with parameter ψ . Furthermore, for each target task τ , KRGTS selects top N_{auxi} auxiliary tasks according to the auxiliary tasks sampling probability. Therefore, each \mathcal{G}_τ consists of a target task, a query molecule, $2K$ support molecules, and N_{auxi} auxiliary tasks, i.e., \mathcal{G}_τ contains $2K+2+N_{\text{auxi}}$ nodes. According to the objective of the auxiliary sampling, it is intuitive to take the value of query loss $\mathcal{L}_{\tau, Q}^{\text{cls}}$ as reward R_{auxi} :

$$\psi \leftarrow \psi + lr_{\text{auxi}} \nabla_\psi P_{\text{auxi}}(R_{\text{auxi}} - b_{\text{auxi}}), \quad (13)$$

where lr_{auxi} is the learning rate of the auxiliary tasks sampler, P_{auxi} is the sampling probability of selected auxiliary tasks, and b_{auxi} is the moving average of reward.

5 Experiments

In this section, extensive experiments are conducted on five well-known benchmark datasets to evaluate the effectiveness of KRGTS with the 10-shot and 1-shot settings. Also, the auxiliary task number experiments, task relevance experiments, and the ablation study are conducted to ensure the effects of each module in KRGTS. Moreover, the details of experiments and more experiment results are listed in Appendix D.

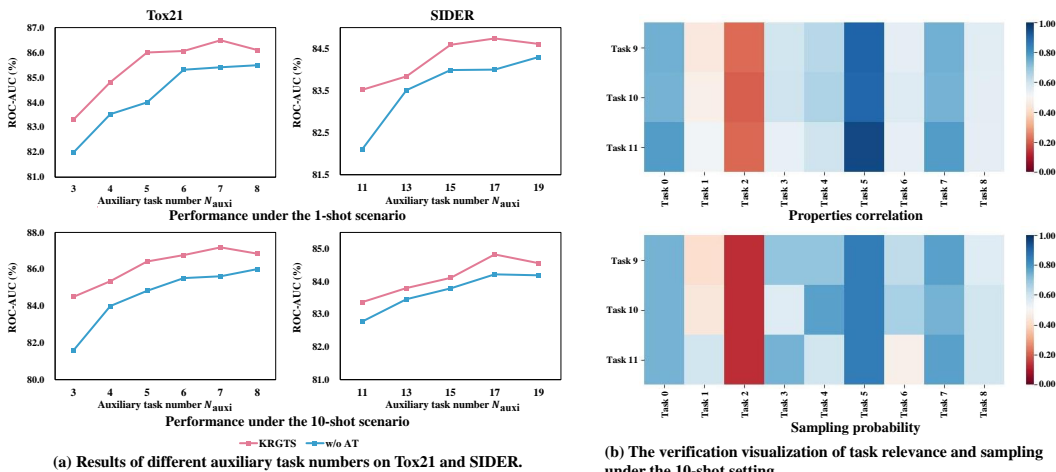


Figure 3: Experiments on the auxiliary task sampler.

5.1 Overall Performance Comparison

Here, following the comparison experiments designed in [10, 26], this paper conducts both the 2-way 10-shot and 2-way 1-shot MPP on Tox21², SIDER [36], MUV [37], ToxCast [38] and PCBA [39]. Table 2 and Table 3 lists the comparison results based on ROC-AUC and standard deviation of KRGTS against 18 well-known baselines. Based on the observations in Table 2 and Table 3 among meta-learning methods, graph neural network methods, and other FSMPP methods, it is evident that KRGTS consistently achieves the best performance in terms of ROC-AUC and its standard deviation on Tox21, SIDER, ToxCast, and PCBA. Specifically, KRGTS outperforms the sub-optimal baselines by 6.17% on PCBA, and particularly achieves 87.62% ROC-AUC on Tox21 in the 10-shot setting. This superior performance can be credited to its ability to capture the many-to-many relationships between molecules and properties. On the MUV dataset with the 10-shot setting, KRGTS performs less effectively than ADKF-IFT. According to the dataset statistics in Appendix D, this phenomenon may be attributed to the sparsity of property labels for MUV molecules, which impacts the model performance. Moreover, the performance of KRGTS on other datasets and the MUV dataset in the 1-shot setting is far superior to ADKF-IFT.

5.2 Analysis of Auxiliary Task Sampler

To delve into the practical effect of auxiliary tasks and the auxiliary task sampler in FSMPP, this study conducts detailed investigations around two questions: **(RQ1)** Should the number of auxiliary tasks be maximized? **(RQ2)** Can the auxiliary task sampler consistently boost model performance under different numbers of auxiliary tasks? With this aim, this subsection compares the performance of KRGTS’s auxiliary task sampler with the random sampler based on various numbers of auxiliary task settings on the Tox21 and SIDER datasets.

As illustrated in Figure 3 (a), the experiment results reveal several important findings: Firstly, as the number of auxiliary tasks gradually increases, the overall model performance shows an upward trend. However, when the number of auxiliary tasks exceeds a certain threshold, the model performance begins to decline; secondly, regardless of how the number of auxiliary tasks is set, the KRGTS auxiliary task sampler consistently demonstrates superior performance compared to the random sampler. Based on these experiment phenomenons, it is easy to conclude that: 1) There exists a balance point for the number of auxiliary tasks, beyond which excessive auxiliary tasks may introduce noise and lead to a decrease in model performance; 2) KRGTS effectively captures relationships between tasks and improves prediction performance through intelligent sampling strategies.

²<https://tripod.nih.gov/tox21/challenge/>

5.3 Analysis of Task Relevance

Capturing task relevance is one of the key characteristics of KRGTS. To verify the task relevance capture ability of the auxiliary task sampler, the relationships of properties and the sampling probability of the auxiliary task sampler on Tox21 under the 2-way 10-shot setting are visualized in Figure 3 (b). Specifically, the properties correlations are Pearson correlation coefficients calculated by task-centered subgraph embeddings acquired from the model after sufficient iterations, where tasks 9-11 are the test set T_{test} of Tox21, and tasks 0-8 are the training set T_{train} . KRGTS speculated that auxiliary properties having high-related scores with the target properties would be more beneficial for the target properties prediction. The sampling probability heatmap corresponds to the output of the auxiliary task sampler when sampling auxiliary tasks from tasks 0-8 for target tasks 9-11. As is shown in Figure 3, it is observed that candidate auxiliary tasks having high-related scores regarding the target tasks are always assigned with higher sampling probabilities, demonstrating that KRGTS can effectively capture the correlation of different properties and sample beneficial auxiliary tasks to improve the property prediction performance.

5.4 Ablation Study

In this part, to further analyze the contribution of KRGTS, the ablation study is conducted on Tox21 with the ablation of each component of KRGTS. Specifically, the ablation experiments include: (1) **w/o S**: without the scaffold similarity relation between molecules, (2) **w/o G**: without using the functional group similarity relation between molecules, (3) **w/o S & G**: without using the relation between molecules, (4) **w/o MT**: randomly select meta-training tasks, (5) **w/o AT**: randomly select auxiliary tasks, (6) **w/o MT & AT**: randomly select meta-training tasks and auxiliary tasks.

Table 4 lists the experimental results of all variants of KRGTS on the Tox21 dataset. Overall, KRGTS significantly outperforms all its variants, which undoubtedly demonstrates the complementarity and indispensability of each module in KRGTS. Specifically, for the knowledge-enhanced molecule-property relation graph module, relying solely on a single similarity relationship leads to a significant drop in performance. The performance degradation is most noticeable when relationships between molecules are not used. Despite this, the variants still maintain competitiveness compared with most baselines, which highlights the contribution of fine-grained similarity relationships between molecules. Furthermore, variants based on samplers exhibit decreased performance, emphasizing the importance of capturing property relationships in property prediction. Among them, the auxiliary task sampler has a more significant impact than the meta-training task sampler. This phenomenon may be attributed to the fact that the auxiliary task sampler is responsible for sampling auxiliary tasks for the target task, which is directly related to the subgraph.

Table 4: Ablation studies on Tox21.

Method	10-shot	1-shot
w/o S	85.97 _(0.54)	85.58 _(0.25)
w/o G	85.55 _(0.20)	85.58 _(0.13)
w/o S & G	85.36 _(0.37)	84.92 _(0.72)
w/o MT	86.06 _(0.22)	85.43 _(0.40)
w/o AT	85.62 _(0.33)	85.41 _(0.65)
w/o MT & AT	85.01 _(0.74)	85.13 _(0.57)
KRGTS	87.19 _(0.11)	86.49 _(0.18)

6 Conclusion

This paper proposes a novel FSMPP framework KRGTS consisting of a knowledge-enhanced molecule-property relation graph learning module and a task sampling module. Specifically, KRGTS constructs the knowledge-enhanced molecule-property relation graph based on the relation of molecular substructure (scaffold similarity and functional group similarity) to capture the information provided by annotated molecules. To effectively utilize the correlation between tasks, KRGTS designs the meta-training task sampler to schedule the training process for better meta-knowledge accumulation and the auxiliary task sampler to select auxiliary tasks having high-related scores with target tasks for more effective property prediction. Comprehensive experiments exhibit the superiority of the KRGTS among the state-of-the-art methods. Also, extra experiment results demonstrate the effectiveness of KRGTS and the contribution of the molecular-property relation graph, the meta-training task sampler as well as the auxiliary task sampler.

However, since molecules are highly complex entities, how to effectively capture the relationships between molecules in the molecule-property relation graph still needs to be optimized. When faced with a considerable number of candidate auxiliary properties, designing models to adaptively sample

an appropriate number of auxiliary properties for the target task remains challenging. Additionally, besides qualitative MPP, quantitative analysis tasks are also crucial. Therefore, in the future, we plan to explore FSMPP from these several directions.

References

- [1] Sheng Wang, Yuzhi Guo, Yuhong Wang, Hongmao Sun, and Junzhou Huang. Smiles-bert: Large scale unsupervised pre-training for molecular property prediction. In *Proceedings of the 10th ACM International Conference on Bioinformatics, Computational Biology and Health Informatics*, BCB '19, page 429–436, New York, NY, USA, 2019. Association for Computing Machinery.
- [2] Han Li, Dan Zhao, and Jianyang Zeng. Kpgt: Knowledge-guided pre-training of graph transformer for molecular property prediction. In *Proceedings of the 28th ACM SIGKDD Conference on Knowledge Discovery and Data Mining*, KDD '22, page 857–867, New York, NY, USA, 2022. Association for Computing Machinery.
- [3] Zhongkai Hao, Chengqiang Lu, Zhenya Huang, Hao Wang, Zheyuan Hu, Qi Liu, Enhong Chen, and Cheekong Lee. Asgn: An active semi-supervised graph neural network for molecular property prediction. In *Proceedings of the 26th ACM SIGKDD International Conference on Knowledge Discovery & Data Mining*, KDD '20, page 731–752, New York, NY, USA, 2020. Association for Computing Machinery.
- [4] Yisheng Song, Ting Wang, Puyu Cai, Subrota K. Mondal, and Jyoti Prakash Sahoo. A comprehensive survey of few-shot learning: Evolution, applications, challenges, and opportunities. *ACM Comput. Surv.*, 55(13s), jul 2023.
- [5] Wenbin Li, Ziyi Wang, Xuesong Yang, Chuanqi Dong, Pinzhao Tian, Tiexin Qin, Jing Huo, Yinghuan Shi, Lei Wang, Yang Gao, and Jiebo Luo. Libfewshot: A comprehensive library for few-shot learning. *IEEE Transactions on Pattern Analysis and Machine Intelligence*, 45(12):14938–14955, 2023.
- [6] Yann Lifchitz, Yannis Avrithis, Sylvaine Picard, and Andrei Bursuc. Dense classification and implanting for few-shot learning. In *2019 IEEE/CVF Conference on Computer Vision and Pattern Recognition (CVPR)*, pages 9250–9259, 2019.
- [7] Xiaoxu Li, Xiaochen Yang, Zhanyu Ma, and Jing-Hao Xue. Deep metric learning for few-shot image classification: A review of recent developments. *Pattern Recognition*, 138:109381, 2023.
- [8] Han Altae-Tran, Bharath Ramsundar, Aneesh S Pappu, and Vijay Pande. Low data drug discovery with one-shot learning. *ACS central science*, 3(4):283–293, 2017.
- [9] Zhichun Guo, Chuxu Zhang, Wenhao Yu, John Herr, Olaf Wiest, Meng Jiang, and Nitesh V. Chawla. Few-shot graph learning for molecular property prediction. In *Proceedings of the Web Conference 2021, WWW '21*, page 2559–2567, New York, NY, USA, 2021. Association for Computing Machinery.
- [10] Yaqing Wang, Abulikemu Abuduweili, Quanming Yao, and Dejing Dou. Property-aware relation networks for few-shot molecular property prediction. In M. Ranzato, A. Beygelzimer, Y. Dauphin, P.S. Liang, and J. Wortman Vaughan, editors, *Advances in Neural Information Processing Systems*, volume 34, pages 17441–17454. Curran Associates, Inc., 2021.
- [11] Wei Ju, Zequn Liu, Yifang Qin, Bin Feng, Chen Wang, Zhihui Guo, Xiao Luo, and Ming Zhang. Few-shot molecular property prediction via hierarchically structured learning on relation graphs. *Neural Networks*, 163:122–131, 2023.
- [12] Lianwei Zhang, Dongjiang Niu, Beiyi Zhang, Qiang Zhang, and Zhen Li. Property-guided few-shot learning for molecular property prediction with dual-view encoder and relation graph learning network. *IEEE Journal of Biomedical and Health Informatics*, 2024.
- [13] Xiang Zhuang, Qiang Zhang, Bin Wu, Keyan Ding, Yin Fang, and Huajun Chen. Graph sampling-based meta-learning for molecular property prediction. In Edith Elkind, editor, *Proceedings of the Thirty-Second International Joint Conference on Artificial Intelligence, IJCAI-23*, pages 4729–4737. International Joint Conferences on Artificial Intelligence Organization, 8 2023. Main Track.

- [14] Tianyi Jiang, Zeyu Wang, Wenchao Yu, Jinhuan Wang, Shanqing Yu, Xiaoze Bao, Bin Wei, and Qi Xuan. Mix-key: graph mixup with key structures for molecular property prediction. *Briefings in Bioinformatics*, 25(3):bbae165, 2024.
- [15] Aleksandr Noy, C Daniel Frisbie, Lawrence F Rozsnyai, Mark S Wrighton, and Charles M Lieber. Chemical force microscopy: exploiting chemically-modified tips to quantify adhesion, friction, and functional group distributions in molecular assemblies. *Journal of the American Chemical Society*, 117(30):7943–7951, 1995.
- [16] Anne-Marie Caminade, Séverine Fruchon, Cédric-Olivier Turrin, Mary Poupot, Armelle Ouali, Alexandrine Maraval, Matteo Garzoni, Marek Maly, Victor Furer, Valeri Kovalenko, et al. The key role of the scaffold on the efficiency of dendrimer nanodrugs. *Nature communications*, 6(1):7722, 2015.
- [17] Qiannan Zhang, Shichao Pei, Qiang Yang, Chuxu Zhang, Nitesh V Chawla, and Xiangliang Zhang. Cross-domain few-shot graph classification with a reinforced task coordinator. In *Proceedings of the AAAI Conference on Artificial Intelligence*, volume 37, pages 4893–4901, 2023.
- [18] W Patrick Walters and Regina Barzilay. Applications of deep learning in molecule generation and molecular property prediction. *Accounts of chemical research*, 54(2):263–270, 2020.
- [19] Evan N Feinberg, Debnil Sur, Zhenqin Wu, Brooke E Husic, Huanghao Mai, Yang Li, Saisai Sun, Jianyi Yang, Bharath Ramsundar, and Vijay S Pande. Potentialnet for molecular property prediction. *ACS central science*, 4(11):1520–1530, 2018.
- [20] Adrià Cereto-Massagué, María José Ojeda, Cristina Valls, Miquel Mulero, Santiago Garcia-Vallvé, and Gerard Pujadas. Molecular fingerprint similarity search in virtual screening. *Methods*, 71:58–63, 2015. Virtual Screening.
- [21] Ingo Muegge and Prasenjit Mukherjee. An overview of molecular fingerprint similarity search in virtual screening. *Expert Opinion on Drug Discovery*, 11(2):137–148, 2016. PMID: 26558489.
- [22] Ying Song, Shuangjia Zheng, Zhangming Niu, Zhang-hua Fu, Yutong Lu, and Yuedong Yang. Communicative representation learning on attributed molecular graphs. In Christian Bessiere, editor, *Proceedings of the Twenty-Ninth International Joint Conference on Artificial Intelligence*, pages 2831–2838. International Joint Conferences on Artificial Intelligence Organization, 7 2020. Main track.
- [23] Xiaomin Fang, Lihang Liu, Jieqiong Lei, Donglong He, Shanzhuo Zhang, Jingbo Zhou, Fan Wang, Hua Wu, and Haifeng Wang. Geometry-enhanced molecular representation learning for property prediction. *Nature Machine Intelligence*, 4(2):127–134, 2022.
- [24] Zeyu Wang, Tianyi Jiang, Jinhuan Wang, and Qi Xuan. Multi-modal representation learning for molecular property prediction: Sequence, graph, geometry. *arXiv preprint arXiv:2401.03369*, 2024.
- [25] Shuangli Li, Jingbo Zhou, Tong Xu, Dejing Dou, and Hui Xiong. Geomgcl: Geometric graph contrastive learning for molecular property prediction. In *Proceedings of the AAAI conference on artificial intelligence*, volume 36, pages 4541–4549, 2022.
- [26] Ziqiao Meng, Yaoman Li, Peilin Zhao, Yang Yu, and Irwin King. Meta-learning with motif-based task augmentation for few-shot molecular property prediction. In *Proceedings of the 2023 SIAM International Conference on Data Mining (SDM)*, pages 811–819. SIAM, 2023.
- [27] H. L. Morgan. The generation of a unique machine description for chemical structures—a technique developed at chemical abstracts service. *Journal of Chemical Documentation*, 5(2):107–113, 1965.
- [28] Joseph L. Durant, Burton A. Leland, Douglas R. Henry, and James G. Nourse. Reoptimization of mdl keys for use in drug discovery. *Journal of Chemical Information and Computer Sciences*, 42(6):1273–1280, 2002. PMID: 12444722.
- [29] Chelsea Finn, Pieter Abbeel, and Sergey Levine. Model-agnostic meta-learning for fast adaptation of deep networks. In *Proceedings of the 34th International Conference on Machine Learning - Volume 70, ICML’17*, page 1126–1135. JMLR.org, 2017.
- [30] Michael Schlichtkrull, Thomas N Kipf, Peter Bloem, Rianne Van Den Berg, Ivan Titov, and Max Welling. Modeling relational data with graph convolutional networks. In *The semantic*

- web: 15th international conference, ESWC 2018, Heraklion, Crete, Greece, June 3–7, 2018, proceedings 15, pages 593–607. Springer, 2018.
- [31] Keyulu Xu, Weihua Hu, Jure Leskovec, and Stefanie Jegelka. How powerful are graph neural networks? In *International Conference on Learning Representations*. OpenReview.net, 2019.
 - [32] Adam Paszke, Sam Gross, Francisco Massa, Adam Lerer, James Bradbury, Gregory Chanan, Trevor Killeen, Zeming Lin, Natalia Gimelshein, Luca Antiga, et al. Pytorch: An imperative style, high-performance deep learning library. *Advances in neural information processing systems*, 32, 2019.
 - [33] Zeren Shui and George Karypis. Heterogeneous molecular graph neural networks for predicting molecule properties. In *2020 IEEE International Conference on Data Mining (ICDM)*, pages 492–500, 2020.
 - [34] R Devon Hjelm, Alex Fedorov, Samuel Lavoie-Marchildon, Karan Grewal, Phil Bachman, Adam Trischler, and Yoshua Bengio. Learning deep representations by mutual information estimation and maximization. In *International Conference on Learning Representations*, 2019.
 - [35] Ronald J Williams. Simple statistical gradient-following algorithms for connectionist reinforcement learning. *Machine learning*, 8:229–256, 1992.
 - [36] Michael Kuhn, Ivica Letunic, Lars Juhl Jensen, and Peer Bork. The sider database of drugs and side effects. *Nucleic acids research*, 44(D1):D1075–D1079, 2016.
 - [37] Sebastian G Rohrer and Knut Baumann. Maximum unbiased validation (muv) data sets for virtual screening based on pubchem bioactivity data. *Journal of chemical information and modeling*, 49(2):169–184, 2009.
 - [38] Ann M Richard, Richard S Judson, Keith A Houck, Christopher M Grulke, Patra Volarath, Inthirany Thillainadarajah, Chihae Yang, James Rathman, Matthew T Martin, John F Wambaugh, et al. Toxcast chemical landscape: paving the road to 21st century toxicology. *Chemical research in toxicology*, 29(8):1225–1251, 2016.
 - [39] Yanli Wang, Jewen Xiao, Tugba O Suzek, Jian Zhang, Jiyao Wang, Zhigang Zhou, Lianyi Han, Karen Karapetyan, Svetlana Dracheva, Benjamin A Shoemaker, et al. Pubchem’s bioassay database. *Nucleic acids research*, 40(D1):D400–D412, 2012.
 - [40] Adam Paszke, Sam Gross, Francisco Massa, Adam Lerer, James Bradbury, Gregory Chanan, Trevor Killeen, Zeming Lin, Natalia Gimelshein, Luca Antiga, Alban Desmaison, Andreas Kopf, Edward Yang, Zachary DeVito, Martin Raison, Alykhan Tejani, Sasank Chilamkurthy, Benoit Steiner, Lu Fang, Junjie Bai, and Soumith Chintala. PyTorch: An Imperative Style, High-Performance Deep Learning Library. In H. Wallach, H. Larochelle, A. Beygelzimer, F. d’Alché Buc, E. Fox, and R. Garnett, editors, *Advances in Neural Information Processing Systems 32*, pages 8024–8035. Curran Associates, Inc., 2019.
 - [41] Gregory Koch, Richard Zemel, Ruslan Salakhutdinov, et al. Siamese neural networks for one-shot image recognition. In *ICML deep learning workshop*, volume 2. Lille, 2015.
 - [42] Jake Snell, Kevin Swersky, and Richard Zemel. Prototypical networks for few-shot learning. In *Proceedings of the 31st International Conference on Neural Information Processing Systems, NIPS’17*, page 4080–4090, Red Hook, NY, USA, 2017. Curran Associates Inc.
 - [43] Yanbin Liu, Juho Lee, Minseop Park, Saehoon Kim, Eunho Yang, Sungju Hwang, and Yi Yang. Learning to propagate labels: Transductive propagation network for few-shot learning. In *International Conference on Learning Representations*, 2019.
 - [44] Jongmin Kim, Taesup Kim, Sungwoong Kim, and Chang D. Yoo. Edge-labeling graph neural network for few-shot learning. In *2019 IEEE/CVF Conference on Computer Vision and Pattern Recognition (CVPR)*, pages 11–20, 2019.
 - [45] Wenlin Chen, Austin Tripp, and José Miguel Hernández-Lobato. Meta-learning adaptive deep kernel gaussian processes for molecular property prediction. *arXiv preprint arXiv:2205.02708*, 2022.
 - [46] Weihua Hu, Bowen Liu, Joseph Gomes, Marinka Zitnik, Percy Liang, Vijay S. Pande, and Jure Leskovec. Strategies for pre-training graph neural networks. In *8th International Conference on Learning Representations, ICLR 2020, Addis Ababa, Ethiopia, April 26-30, 2020*. OpenReview.net, 2020.

- [47] Ruochi Zhang, Chao Wu, Qian Yang, Chang Liu, Yan Wang, Kewei Li, Lan Huang, and Fengfeng Zhou. Molfescue: Enhancing molecular property prediction in data-limited and imbalanced contexts using few-shot and contrastive learning. *Bioinformatics*, page btae118, 2024.

A List of Abbreviations

Here we list the abbreviations of concepts used in this paper.

Table 5: List of Abbreviations.

Abbreviation	Meaning
MPP	Molecular Property Prediction
FSMPP	Few-shot Molecular Property Prediction
MPRG	Molecule-property Relation Graph
MPMRG	Molecule-property Multi-relation Graph

B Algorithm of KRGTS

Algorithm 1 Algorithm of KRGTS

Input: Knowledge-enhanced molecule-property relation graph M

Output: Relation Subgraph Learning Module f_θ , Meta-training task sampler f_ϕ , Auxiliary task sampler f_ψ

for epoch=1, \dots , epochs **do**

 Sample the task pool $\{(\mathcal{G}_t^1, \mathcal{G}_t^2)\}_{t=1}^{N_{\text{pool}}}$ from M .

 Sample $\{(\mathcal{G}_t^1, \mathcal{G}_t^2)\}_{t=1}^{N_{\text{meta}}}$ with f_ϕ .

for $\tau = 1, \dots, N_{\text{meta}}$ **do**

 Sample N_{auxi} auxiliary properties with f_ψ for $\mathcal{G}_\tau^1, \mathcal{G}_\tau^2$.

 Calculate the classification loss of the support set by Equation (7) on $\mathcal{G}_\tau^1, \mathcal{G}_\tau^2$.

 Inner-update the relation subgraph learning module parameters by Equation (14).

 Calculate the classification loss of the query molecules as Equation (7) on $\mathcal{G}_\tau^1, \mathcal{G}_\tau^2$.

end for

 Calculate contrastive loss by Equation (10)

 Outer-update the relation subgraph learning module parameters by Equation (15).

 Update the meta-training task sampler parameters by Equation (11).

 Update the auxiliary task sampler parameters by Equation (13).

end for

As is described in Algorithm 1, the training process involves two loops with the episodic training diagram. Firstly, the meta-training task sampler is utilized to sample N_{meta} meta-training task from the task pool. For each meta-training task training or in the inner loop, the auxiliary task sampler is used to sample N_{auxi} auxiliary properties to assist in target property prediction. The loss of support set will be used to update the relation subgraph learning module parameters θ in the inner loop:

$$\theta \leftarrow \theta - lr_{\text{inner}} \nabla_{\theta} \mathcal{L}_{t,S}^{\text{cls}} \quad (14)$$

where lr_{inner} is the learning rate in inner loop. After the training of N_{meta} meta-training tasks, relation subgraph learning module parameters are updated using the query classification loss and contrastive loss:

$$\theta \leftarrow \theta - lr_{\text{outer}} \nabla_{\theta} (\lambda_{\text{ctr}} \mathcal{L}^{\text{ctr}} + \sum_{t=1}^{N_{\text{meta}}} \mathcal{L}_{t,Q}^{\text{cls}}) \quad (15)$$

where lr_{outer} is the learning rate across the outer loop, and λ_{ctr} is a hyperparameter. Then, the meta-training task sampler and the auxiliary task sampler are updated in order. Among them, considering the diversity of molecular properties, the auxiliary task sampler adopts the batch update to enhance its stability and efficiency.

C Relation Subgraph Learning Module

The embedding of molecules and properties nodes \mathcal{V}, \mathcal{T} can be initialized as:

$$h_i^0 = \begin{cases} f_{\text{mol}}(i) & \text{For } i \in \mathcal{V} \\ \text{Embedding}(i) & \text{For } i \in \{\tau \cup T_{\text{auxi}}\} \end{cases} \quad (16)$$

Table 6: Summary of datasets.

Dataset	Tox21	SIDER	MUV	ToxCast	PCBA
# Compounds	7831	1427	93127	8575	437929
# Tasks	12	27	17	617	128
# Train Tasks	9	21	12	451	118
# Test Tasks	3	6	5	158	10
% Missing Label	17.05	0	84.21	14.97	39.92
% Label <i>active</i>	6.24	56.76	0.31	12.60	0.84
% Label <i>inactive</i>	76.71	43.24	15.76	72.43	59.84

Table 7: Detailed information of sub-datasets on ToxCast dataset.

Sub-dataset	APR	ATG	BSK	CEETOX	CLD	NVS	OT	TOX21	Tanguay
# Compounds	1039	3423	1445	508	305	2130	1782	8241	1039
# Tasks	43	146	115	14	19	139	15	100	18
# Train Tasks	33	106	84	10	14	100	11	80	13
# Test Tasks	10	40	31	4	5	39	4	20	5
% Missing Label	28.09	0.16	0	1.36	0.98	92.27	2.44	8.35	1.11
% Label <i>active</i>	10.30	5.92	17.71	22.26	30.72	3.21	9.78	5.39	8.05
% Label <i>inactive</i>	61.61	93.92	82.29	76.38	68.30	4.52	87.78	86.26	90.84

where $h_i^0 \in \mathbb{R}^d$ is the embedding of node i with dimension d , f_{mol} is a graph encoder [31], and the Embedding is an embedding layer in Pytorch [40]. Different from the node embedding, edge embeddings should incorporate the information of relation types and edge weights. Therefore, KRGTS develops encoding methods tailored to the relationship types and corresponding edge weights. Firstly, the relation types R contain three types: molecule-property relation, scaffold similarity molecules relation, and functional group similarity molecules relation. The embedding of each relation type x_r can be randomly initialized with the same length as molecule embedding by the Embedding layer. Since the edge information is different in the corresponding relation graph, KRGTS designs three types of edge weight encoding methods. Among them, the molecule-property edge weights $B^{\text{Pro}} = \{b_{i,\tau} | (i, \tau) \in E^{\text{Pro}}\}$ contains the label of molecular properties (0 is inactive, 1 is active, 2 is unknown). Similar to the relation type, the embedding of the molecule-property edge weight x_b can be randomly initialized with the same length as molecule embedding by the Embedding layer. While the scaffold similarity molecules edge weights $B^{\text{Sca}} = \{b_{i,j} | (i, j) \in E^{\text{Sca}}\}$ and the functional group similarity molecules edge weights $B^{\text{Gro}} = \{b_{i,j} | (i, j) \in E^{\text{Gro}}\}$ are not integer type ($b_{i,j} \in [0, 1]$), following the previous work [33], KRGTS adopts to two RBF layers with MLP layer to encode diverse molecular similarity:

$$x_{b^{\text{Sca}}} = \text{MLP}(\text{RBF}(b^{\text{Sca}})) \quad (17)$$

$$x_{b^{\text{Gro}}} = \text{MLP}(\text{RBF}(b^{\text{Gro}})) \quad (18)$$

where the dimension of $x_{b^{\text{Sca}}}$ and $x_{b^{\text{Gro}}}$ are same as the molecules embeddings. Then, for each edge (i, j) , one can concatenate the edge relation type embedding x_r and edge weight embedding x_b to get the embedding $h_{i,j}$:

$$h_{i,j} = \sigma(\text{MLP}([x_r \oplus x_b])) \quad (19)$$

where σ is the activation function, \oplus is a concatenation operation, and (i, j) belongs to the G^r .

D Supplementary for Experiments

The comprehensive experiments are conducted on five well-known FSMPP datasets: Tox21, SIDER, MUV, ToxCast, and PCBA. Table 6 shows the detailed statistics of these benchmark datasets. Regarding the data split, Tox21, SIDER, and MUV datasets followed the split settings provided by [8]. For PCBA, the split setting referred to [13]. Additionally, due to the sparsity of ToxCast, the dataset was divided into nine sub-datasets as [13]. As illustrated in Table 7, each sub-dataset corresponds to specific properties.

D.1 Details of Baselines

To conduct a comprehensive comparison, this paper adopts three types of baselines consisting of meta-learning methods, graph neural network methods, and other FSMPP methods. The details of the baselines are as follows:

Methods without Pre-training.

- Siamese [41] utilizes dual convolutional neural networks to identify whether the input samples are from the same class.
- ProtoNet [42] classifies according to the inner-product similarity between the query sample and the prototype of each class.
- MAML [29] learns a model parameter initialization and adapts to new tasks via gradient descent.
- TPN [43] builds a relation graph and utilizes the entire query set for transductive inference.
- EGNN [44] constructs a relation graph and predicts edge labels on the graph.
- IterRefLSTM [8] adapts a modification of Matching Networks for MPP tasks.
- PAR [10] employs a property-aware embedding function and adaptive relation graph learning to effectively propagate information among similar molecules.
- HSL-RG⁻ [11] leverages graph kernels and self-supervised learning to explore the structural semantics from both global-level and local-level granularities.
- GS-Meta [13] constructs a molecule-property relation graph to leverage other available properties and reformulates an episode in meta-learning as a subgraph of this graph.
- ADKF-IFT [45] is a framework for learning deep kernel Gaussian processes through interpolation between traditional deep kernel learning and meta-learning.

Methods with Pre-training

- Pre-GNN [46] is a pre-trained GNN using graph-level and node-level self-supervised tasks and is finetuned using a support set.
- Meta-MGNN [9] uses the Pre-GNN encoder and optimizes with self-supervised tasks in meta-training.
- Pre-PAR [10] is PAR initialized with Pre-GNN.
- HSL-RG [11] is HSL-RG⁻ trained with the initialization of Pre-GNN.
- Pre-GS-Meta [13] is the same as GS-Meta but uses the Pre-GNN encoder.
- Pre-ADKF-IFT [45] is ADKF-IFT that begins with a pre-trained feature extractor.
- MolFeSCue [47] is a few-shot contrastive learning framework that combines the few-shot learning strategy with contrastive learning loss.
- PG-DERN [12] is a few-shot learning model that introduces a dual-view encoder to learn a meaningful molecular representation by integrating information from node and subgraph.

D.2 Implementation Details

KRGTS is implemented in PyTorch [32] on a Ubuntu Server equipped with Intel(R) Core(TM) i7-8700K CPU, and 2 NVIDIA GeForce GTX 1080 Ti (with 11GB memory each). The experiments were conducted over 2000 training epochs based on Adam optimizer, with testing performed every 50 epochs, and repeated for 5 random runs on 2-way K -shot learning tasks, where $K \in \{1, 10\}$. Specifically, for the knowledge-enhanced molecule-property relation graph learning module, the following settings were used: (1) 9 and 1 top- k molecule similarity preserved in subgraphs for 10-shot and 1-shot experiments, respectively; (2) a 5-layer GIN with a hidden size of 300 was employed as the graph-based molecular encoder; (3) the subgraph learning module consisted of a 2-layer GNN and a classifier comprising 2 layers MLP. For the meta-training task sampler, the task pool size N_{pool} was set to 10, and the number of meta-training tasks sampled N_{meta} was set to 5. The function f_{meta} was implemented as a single-layer MLP. As for the auxiliary task sampler, f_{auxi} was configured as a sequential module consisting of 2 layers MLP. Moreover, the rest parameters are listed in Table 8. And the number of auxiliary tasks on each dataset is listed in Table 9 and Table 10.

Table 8: Parameters in implementation.

Description	Value
The dimension of embedding	300
The hidden size of classifier	100-300
The hidden size of meta-training task sampler	300
The hidden size of auxiliary task sampler	300
The learning rate of the inner loop	0.01-1
The learning rate of the outer loop	0.001
The learning rate of meta-training task sampler	0.0005
The learning rate of auxiliary task sampler	0.0005
The dropout rate in molecular encoder	0.1-0.5
The dropout rate in the subgraph encoder	0.1-0.5
The contrastive loss weight in the outer loop	0.05
The temperature parameter of contrastive loss	0.05

Table 9: The number of auxiliary tasks on Tox21, SIDER, MUV and PCBA dataset.

Dataset	Tox21	SIDER	MUV	PCBA
The number of auxiliary tasks of 1-shot	7	17	2	20
The number of auxiliary tasks of 10-shot	7	17	2	20

Table 10: The number of auxiliary tasks on ToxCast dataset.

Sub-dataset	APR	ATG	BSK	CEETOX	CLD	NVS	OT	TOX21	Tanguay
The number of auxiliary tasks of 1-shot	16	12	17	8	12	20	7	18	11
The number of auxiliary tasks of 10-shot	16	12	17	8	12	20	7	18	11

Table 11: Performance on each sub-dataset of ToxCast in the 1-shot scenario.

Method	APR	ATG	BSK	CEETOX	CLD	NVS	OT	TOX21	Tanguay
MAML	64.59	55.45	60.36	61.02	66.22	59.84	62.15	59.52	60.92
ProtoNet	57.08	54.92	53.92	60.25	66.25	54.87	63.11	58.27	58.32
EGNN	67.06	57.28	60.82	60.10	71.53	56.56	66.08	63.32	74.80
PAR	74.24	63.48	70.41	61.44	75.76	67.56	65.72	68.94	77.54
GS-Meta	<u>87.90</u>	<u>79.62</u>	<u>85.94</u>	<u>67.49</u>	<u>78.16</u>	<u>71.04</u>	<u>72.36</u>	<u>87.84</u>	<u>89.97</u>
KRGTS	89.11	79.80	86.36	70.09	80.46	75.20	73.98	88.19	91.68
Pre-PAR	84.69	70.38	79.89	66.57	77.83	72.51	70.41	80.33	86.64
Pre-GS-Meta	89.49	81.69	87.28	<u>68.55</u>	<u>78.66</u>	<u>74.36</u>	<u>73.56</u>	<u>89.46</u>	<u>91.10</u>
Pre-KRGTS	<u>89.45</u>	<u>79.54</u>	<u>86.84</u>	72.50	81.21	76.63	73.68	89.51	92.15

Table 12: Performance on each sub-dataset of ToxCast in the 10-shot scenario.

Method	APR	ATG	BSK	CEETOX	CLD	NVS	OT	TOX21	Tanguay
MAML	72.66	62.09	66.42	64.08	74.57	66.56	64.07	68.04	77.12
ProtoNet	73.58	59.26	70.15	66.12	78.12	65.85	64.90	68.26	73.61
EGNN	80.33	66.17	73.43	66.51	78.85	71.05	68.21	76.40	85.23
PAR	82.74	68.86	74.65	67.76	78.33	70.79	69.12	77.34	83.39
GS-Meta	<u>88.95</u>	80.44	87.67	<u>69.50</u>	<u>79.95</u>	<u>74.77</u>	<u>73.46</u>	<u>88.78</u>	<u>90.48</u>
KRGTS	89.95	<u>80.30</u>	<u>87.22</u>	72.15	81.25	76.84	74.63	89.19	91.96
Pre-PAR	86.09	72.72	82.45	72.12	83.43	74.94	71.96	82.81	88.20
Pre-GS-Meta	<u>90.15</u>	82.54	88.21	<u>74.19</u>	<u>86.34</u>	<u>76.29</u>	<u>74.47</u>	90.63	<u>91.47</u>
Pre-KRGTS	90.31	<u>80.12</u>	<u>87.92</u>	76.63	86.97	77.52	75.11	<u>89.83</u>	91.73

D.3 Performance of ToxCast Sub-datasets

Consistent with [13], each sub-dataset was further divided into meta-training and testing sets, as illustrated in Table 7. The results of the sub-datasets are presented in Table 11 and Table 12. Also, the results in Table 2 and Table 3 are averaged from Table 11 and Table 12. From the experimental results, it can be observed that KRGTS shows significant gains on most sub-datasets, leading to an overall performance improvement on the entire dataset, further demonstrating the effectiveness of KRGTS.

D.4 Computation Resource Analysis

To conduct a comprehensive performance evaluation, we compared the time complexity of KRGTS with GS-Meta. Specifically, considering that the runtime of KRGTS is primarily influenced by subgraph learning in the sampler, we selected three datasets (MUV, Tox21, SIDER) with different scales and recorded the training time and memory consumption for each epoch

on each dataset. The experimental results are presented in Table 3. Overall, KRGTS significantly outperforms GS-Meta in terms of performance and memory consumption, especially in cases of sparse labels, where it shows impressive superiority in performance and runtime. Additionally, we observed that the runtime of KRGTS is affected by the number of candidate auxiliary tasks. For instance, KRGTS exhibits the fastest runtime on the MUV dataset, which has the sparsest labels. Although the time complexity increases on the Tox21 and SIDER datasets due to their relatively denser labels, this issue can be effectively mitigated by employing a multi-process training mechanism.

Table 13: Time complexity comparison.

Dataset	GS-Meta	KRGTS
Tox21	85.85%(2.37s, 6030MB)	87.19% (3.10s, 3134MB)
SIDER	83.72%(2.45s, 7674MB)	84.83% (5.23s, 4780MB)
MUV	67.11%(2.47s, 6302MB)	72.63% (1.63s, 4598MB)